COMPRESSIVE DEFORMATION BEHAVIOUR OF ALSI10MG MICROLATTICE STRUCTURES BY SELECTIVE LASER MELTING

NINIAN S.K. HO[1], PEIFENG LI[2] AND GIN B. CHAI[3]

[1]School of Mechanical and Aerospace Engineering, Nanyang Technological University, 50 Nanyang Avenue, Singapore 639798
ho0009an@e.ntu.edu.sg

[2]School of Engineering, University of Glasgow, James Watt South Building, Glasgow G12 8QQ, UK
peifeng.li@glasgow.ac.uk

[3]School of Mechanical and Aerospace Engineering, Nanyang Technological University, 50 Nanyang Avenue, Singapore 639798
mgbchai@ntu.edu.sg

Key words: Finite Element Model, Deformation, Microlattice Structures, Selective Laser Melting.

Abstract. Understanding the mechanical performance of microlattice structures requires the detailed analysis of the localised stress distribution and deformation process. In this study, a finite element (FE) model was developed to simulate the compressive deformation behaviour of AlSi10Mg microlattice structures manufactured by selective laser melting (SLM). The constitutive properties of the SLM AlSi10Mg were experimentally measured in uniaxial tension tests and formulated by the Johnson–Cook model. The FE simulation was validated by uniaxial compression tests of SLM microlattices, and provided the valuable insight into the damage evolution in the microlattices. The predicted localised deformation may explain the formation of the 45° shear band observed experimentally in the microlattices. Further work will be carried out to include the description of damage in the constitutive model of SLM AlSi10Mg alloys in order to accurately predict the localised damage evolution in the struts of the microlattices.

1 INTRODUCTION

Metallic microlattice structures are promising porous materials for lightweight components as well as shock absorption, heat exchange and sound absorption applications [1-3]. For a given weight, they are stronger than stochastic metallic foams due to their geometrically periodic nature [4]. Metallic microlattices can be simply viewed as improved versions of such foams. Ultralight microlattice structures have been developed for future aerospace vehicles [5], demonstrating their potential for aerospace applications alone.

Selective laser melting (SLM) is an additive manufacturing (AM) technique based on the powder bed fusion process [6]. As expected of AM techniques in general, the SLM can produce near net shape parts and allows for greater geometrical flexibility. Thus it has been used to manufacture microlattice structures of complex unit cell topologies using various

metal powders such as stainless steel, titanium alloys and aluminium alloys [7-9]. AlSi10Mg is the most commonly used alloy among the aluminium alloys that have been successfully translated to the SLM process [10]. Mechanical properties of SLM AlSi10Mg have been shown to be on par with, if not superior to, those of conventionally cast AlSi10Mg alloys [11].

The mechanical properties of SLM metallic microlattices have been widely studied, in particular the modulus and strength under quasi-static compression [3, 4, 7, 8]. The deformation and failure modes of the microlattices were also been documented in the literature. While a wealth of experimental data exists in this respect, little effort has been made to quantitatively characterise the compressive properties of these microlattices in general by exploiting their geometrically periodic nature. Most studies reported observations qualitatively that are likely specific to individual types of microlattices, taking a macro-scale approach much like in the case of stochastic cellular materials. As such, there is still limited information pertaining to the compressive deformation behaviour of these microlattices. It is also important to differentiate between laterally (i.e., normal to the loading direction) constrained and unconstrained microlattices, as the former involves boundary conditions that differ across the unit cells in a microlattice depending on their relative positions [7, 8], while for the latter there is no reason for the unit cell boundary conditions to vary across the horizontal plane.

Numerical modelling using finite element (FE) method has been a typical component of investigations on the mechanical properties of microlattice structures. Strut diameter [12], parent material properties (both elastic and plastic) [8, 13] and friction coefficient [14] are parameters that have proven difficult to obtain to be input into FE simulations. In most cases, one of them is fitted such that the numerical predictions match experimental results or has its relevant parameter values assumed.

The aim of this study reported here is to understand the uniaxial compressive deformation behaviour of microlattice structures using FE modelling. Uniaxial tension tests on SLM AlSi10Mg alloys were conducted to develop the parent material constitutive equation for the FE model. It is hoped that new insights gathered could be used to improve the FE modelling of such structures.

2 METHODOLOGY

2.1 Selective laser melting

AlSi10Mg solid cylinders and microlattice structures were manufactured in an SLM-250HL selective laser melting system (SLM Solutions GmbH, Germany). The microlattice structure consisted of 4×4×5 body centred cubic (BCC) unit cells. The nominal strut diameter and unit cell size of the microlattice were $d = 330\,\mu m$ and $L = 3.0$ mm respectively (Figure 1). The solid cylinders were printed horizontally whilst the microlattice specimens were built along their height (measuring 5 unit cells). The laser power was 350 W, the scanning speed was 1150 mm s^{-1}, the layer thickness was 50 µm, and the hatch spacing was 170 µm achieved with a "stripes" pattern. All specimens were subsequently removed from the substrate plates via electrical discharge machining (EDM).
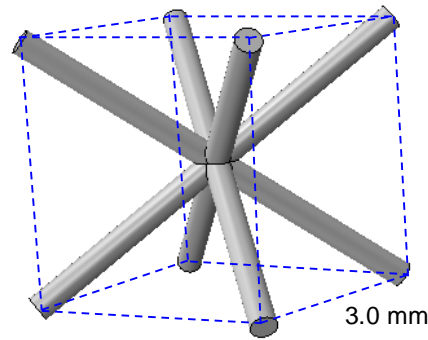
Figure 1: A representative body centred cubic unit cell in microlattice structures.

2.2 Uniaxial tension testing of SLM AlSi10Mg specimens

Each of the solid cylinders was machined into a tension test specimen according to ASTM E8 standards, with a gauge section of length 30 mm and diameter 5 mm. Uniaxial tension tests were performed on the specimens in an INSTRON 5569 (INSTRON, MA, USA) electromechanical universal testing machine. An extensometer with a gauge length of 25 mm was used in conjunction with a 50 kN load cell. The crosshead speed was 0.45 mm min^{-1}, and the extensometer recorded the strain values up to the point of fracture.

2.3 Uniaxial compression testing of SLM AlSi10Mg microlattice structures

Due to the EDM process, each of the SLM microlattice structures comprised 4×4×4.5 BCC unit cells. Uniaxial compression tests on the microlattice specimens along the SLM build direction were carried out in the INSTRON machine in conjunction with a 5 kN load cell. Araldite Rapid epoxy adhesive was used to bond the top and bottom surfaces of each specimen to 316L cylindrical solid blocks to prevent lateral sliding of the struts located there. Curing of the epoxy was done overnight at room temperature and pressure. A crosshead speed corresponding to a strain rate of 0.001 s^{-1} was applied, and strain measurements were obtained from the crosshead readings.

2.4 Finite element modelling of microlattice structures under compression

Finite element modelling was performed using ABAQUS (Dassault Systèmes Simulia Corp., RI, USA) to study the deformation behaviour of the microlattice with 4×4×4.5 BCC unit cells subjected to quasi-static uniaxial compression. The geometrical model of the microlattice was generated using idealised struts. Given the inherent difficulty in determining the effective diameter of SLM struts, a parametric study was conducted to investigate how varying the strut diameter would affect the stress–strain response of microlattices. The diameters of random struts were measured with a digital calliper, and variations were large with values typically between 500 and 600 µm. Thus three strut diameters were chosen in this parametric study, which were d = 500, 600 and 700 µm. Quadratic tetrahedral FE elements were used to mesh the microlattices. The same boundary and loading conditions were applied to all the three simulations. Two plates were added to the top and bottom surfaces of the FE models to constrain them laterally. The bottom surface of the bottom plate in each simulation was fixed while the top surface of the top plate was loaded with a displacement.

3

3 RESULTS AND DISCUSSION

3.1 Constitutive equation of SLM AlSi10Mg alloys

Figure 2(a) shows the nominal stress–strain curves of SLM AlSi10Mg alloys obtained from the tension tests. The Johnson–Cook (J–C) constitutive model was used to relate the true stress (σ) and true plastic strain (ε_{pl}):

$$\sigma = A + B\,\varepsilon_{pl}{}^{n} \tag{1}$$

where the material constants $A = 231$ MPa, $B = 1030$ MPa and $n = 0.4711$ were determined from the experimentally measured curve (Figure 2(b)). The J–C constitutive equation of the SLM AlSi10Mg was input into the FE simulations.
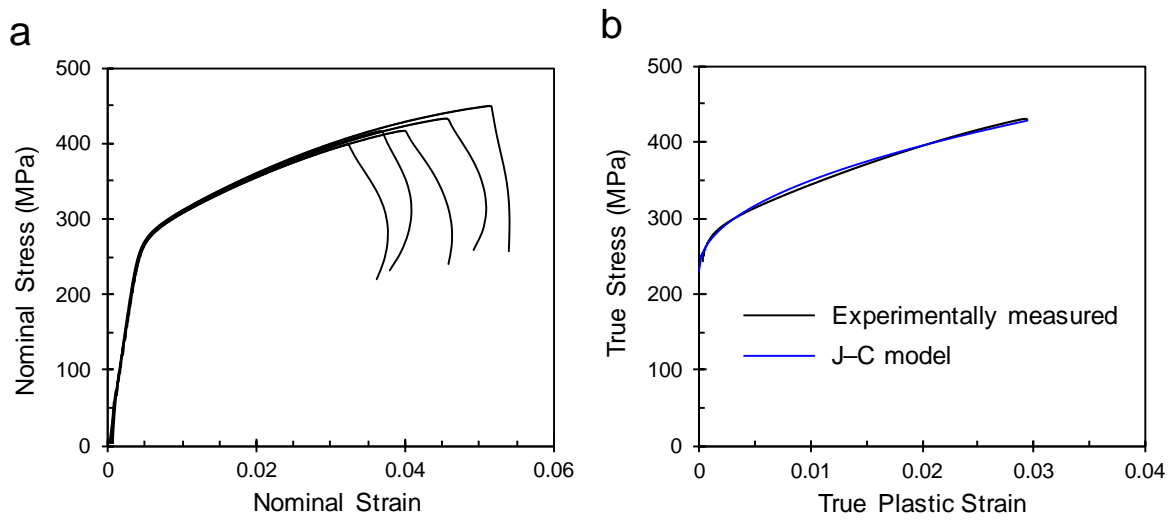

Figure 2: (a) Nominal stress–strain curves of SLM AlSi10Mg alloys and (b) the J–C hardening model fitted from the measured stress–strain data.

3.2 Deformation behaviour of microlattice structures

The experimentally measured stress–strain curves of microlattice structures are shown in Figure 3. A 45° shear band was also observed in the tested microlattice specimens. Figure 3 also illustrates the predicted curves of idealised microlattices with different strut diameters. The FE results of the microlattice with $d = 500\ \mu$m was found to almost coincide with the experimental stress–strain curves prior to the stress drop. This indicates that there was excellent agreement between the numerical predictions and experimental measurements. Based on accurate characterisation of the density of the bulk AlSi10Mg parent material and the microlattices, the average effective strut diameter of the microlattices was determined to be 527 μm (deviating from the nominal diameter 330 μm input for the SLM fabrication process) which is very close to the input diameter of 500 μm in the FE simulation.

The FE model was re-run on the microlattice with $d = 500\ \mu$m with an extension of the final nominal strain up to 0.5. A general interaction was introduced for all the surfaces (all with self) whereby contact properties were defined with a penalty friction formulation

(ballpark friction coefficient 0.1) for tangential behaviour and a "hard" contact for normal behaviour.
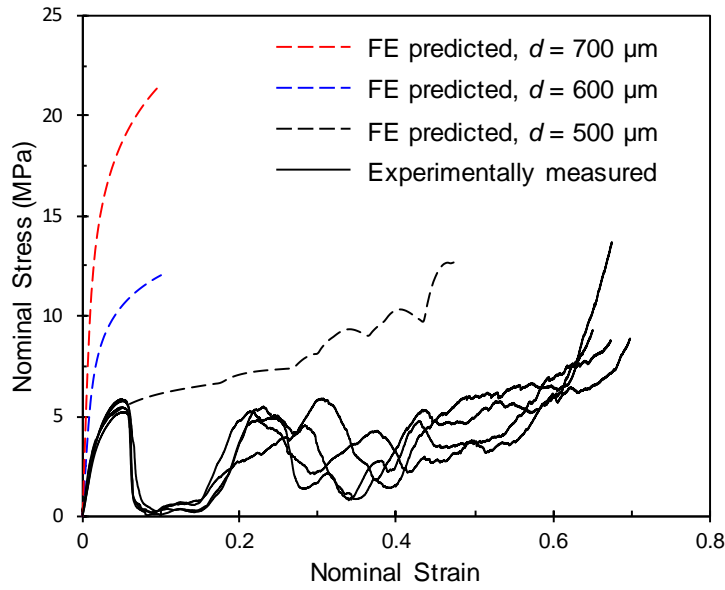

Figure 3: Comparison between the FE predicted and experimentally measured stress–strain curves of the SLM AlSi10Mg microlattice structures.
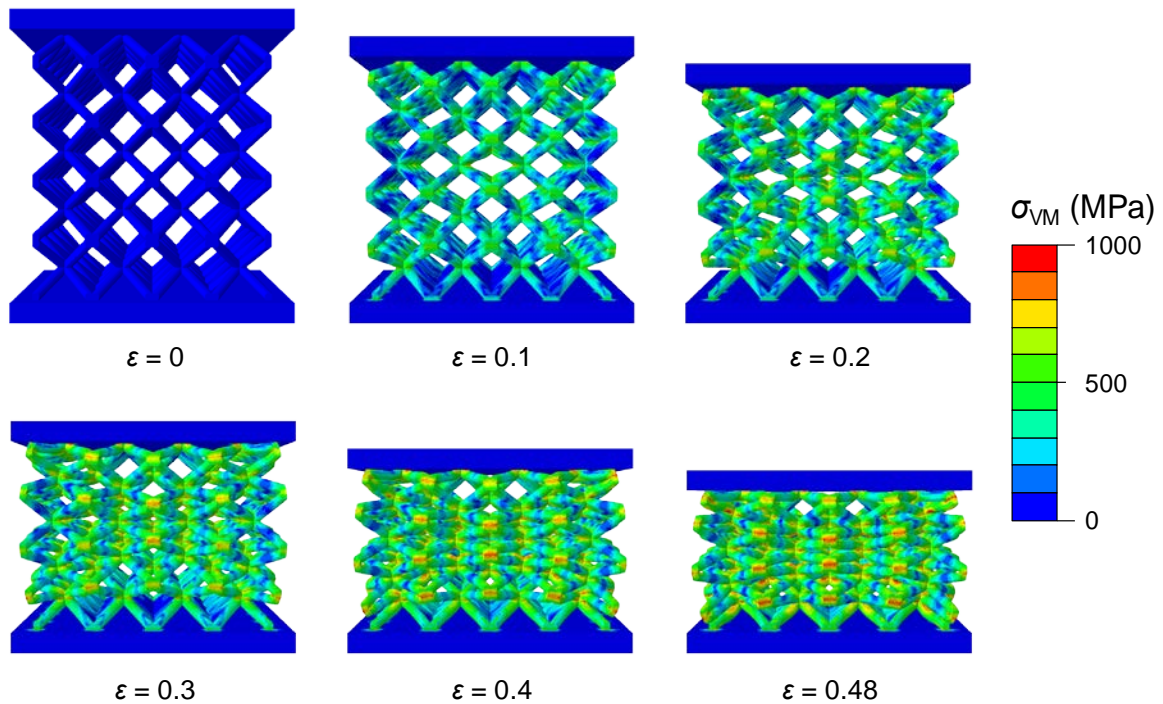

Figure 4: Predicted von Mises stress distribution and deformation process at different strain stages in the uniaxial compression of a microlattice structure with 4×4×4.5 BCC unit cells and strut diameter $d = 500$ µm. The free face of the microlattice is shown in the front view.

5

The stress–strain curve and deformation process of the microlattices as predicted by the final FE model are shown in Figures 3 and 4 respectively. However, the 45° shear band was not predicted in the simulation. The predicted localised von Mises stress in struts can reach 1000 MPa (see Figure 4) that is greater than the failure strength of SLM AlSi10Mg (Figure 2). Moreover, the predicted curve is above the experimentally measured curve (Figure 3). These inconsistencies arose because the material damage was not included in the model.

A close inspection of the stress distributions in the microlattice reveals that stress concentrates at the nodes, as opposed to the struts (Figure 4). Due to the barrelling effect as observed, the microlattice bulges outwards, such that only the cross-sections exactly halving the microlattices remain plane throughout the deformation process, with all other cross-sections becoming more and more convex with respect to the midplanes of the microlattice (Figure 5).

Within a laterally constrained microlattice, different nodes undergo different stress levels depending on their relative positions within the microlattice (Figures 4 and 5). This is due to the varying boundary conditions across the individual unit cells. Different non-uniform deformation patterns were observed on different cross-sections in the microlattice. A roughly "X" shaped crush band forms gradually with the topmost and bottom-most layers of unit cells deforming last. Within these bands, a crack will form in a strut first due to the geometrical imperfections introduced by the SLM process, breaking the symmetry of the deformation and thus resulting in a 45° shear band.
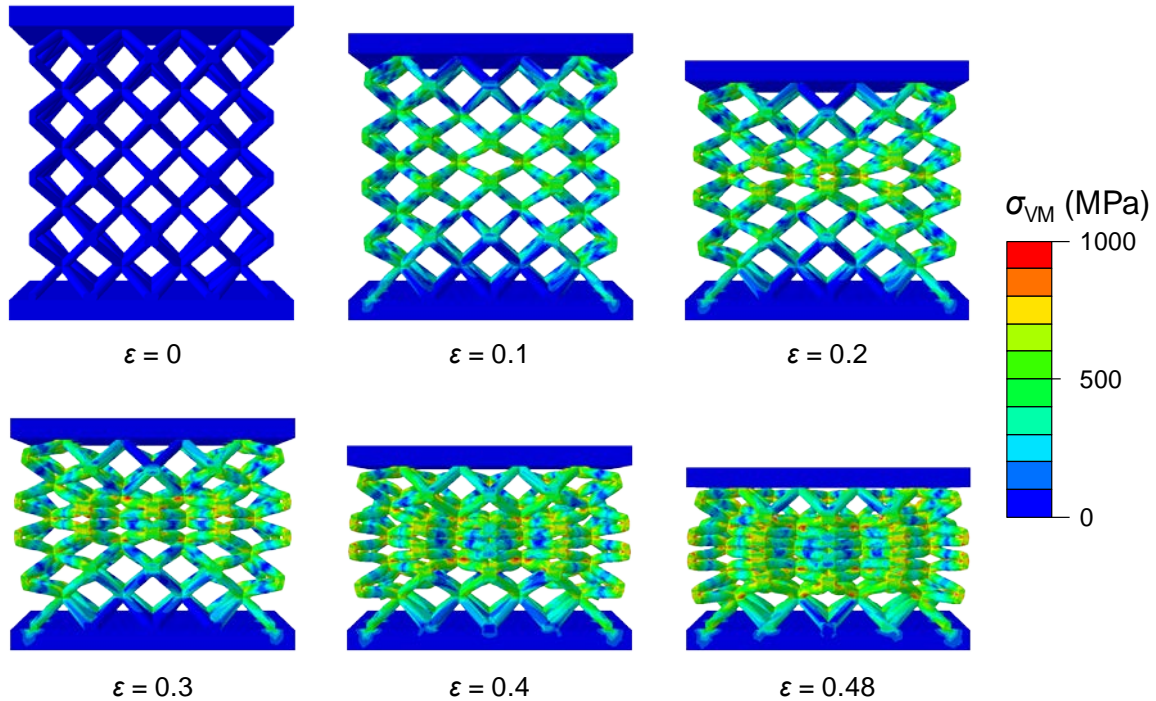

Figure 5: Predicted von Mises stress distribution and deformation process in the rear half (two unit cell layers) of a microlattice structure at different strain stages in the uniaxial compression. The midplane of the microlattice is shown in the front view.

4   CONCLUSIONS

- The constitutive behaviour of SLM AlSi10Mg alloys can be quantified using J–C hardening model. FE modelling with this J–C constitutive equation can accurately predict the deformation behaviour of idealised microlattice structures under compression prior to the initial stress drop. Further work will incorporate the damage in the material data.
- The predicted localised deformation may explain the formation of the 45° shear band observed experimentally. The FE simulation suggests that microlattice structures can be strengthened by adding more materials to their nodes.

REFERENCES

[1] Li, P. Constitutive and failure behaviour in selective laser melted stainless steel for microlattice structures. *Mater. Sci. Eng. A* (2015) **622**:114-120.

[2] Rehme, O. and Emmelmann, C. Rapid manufacturing of lattice structures with selective laser melting, in *Lasers and Applications in Science and Engineering*, SPIE, 2006, pp. 12.

[3] Van Bael, S., Kerckhofs, G., Moesen, M., Pyka, G., Schrooten, J. and Kruth, J.P. Micro-CT-based improvement of geometrical and mechanical controllability of selective laser melted Ti6Al4V porous structures. *Mater. Sci. Eng. A* (2011) **528**:7423-7431.

[4] Feng, Q., Tang, Q., Liu, Z., Liu, Y. and Setchi, R. An investigation of the mechanical properties of metallic lattice structures fabricated using selective laser melting. *Proc. Inst. Mech. Eng. B* (2016).

[5] Schaedler, T.A., Jacobsen, A.J., Torrents, A., Sorensen, A.E., Lian, J., Greer, J.R., Valdevit, L. and Carter, W.B. Ultralight metallic microlattices. *Science* (2011) **334**:962-965.

[6] Do, D.K. and Li, P. The effect of laser energy input on the microstructure, physical and mechanical properties of Ti-6Al-4V alloys by selective laser melting. *Virtual Phys. Prototyp.* (2016) **11**:41-47.

[7] Leary, M., Mazur, M., Elambasseril, J., McMillan, M., Chirent, T., Sun, Y., Qian, M., Easton, M. and Brandt, M. Selective laser melting (SLM) of AlSi12Mg lattice structures. *Mater. Des.* (2016) **98**:344-357.

[8] Li, P., Wang, Z., Petrinic, N. and Siviour, C.R. Deformation behaviour of stainless steel microlattice structures by selective laser melting. *Mater. Sci. Eng. A* (2014) **614**:116-121.

[9] Wang, Z. and Li, P. Characterisation and constitutive model of tensile properties of selective laser melted Ti-6Al-4V struts for microlattice structures. *Mater. Sci. Eng. A* (2018) **725**:350-358.

[10] Leon, A., Shirizly, A. and Aghion, E. Corrosion behavior of AlSi10Mg alloy produced by additive manufacturing (AM) vs. its counterpart gravity cast alloy. *Metals* (2016) **6**:148.

[11] Kempen, K., Thijs, L., Van Humbeeck, J. and Kruth, J.P. Mechanical properties of AlSi10Mg produced by selective laser melting. *Phys. Procedia* (2012) **39**:439-446.

[12] Cansizoglu, O., Harrysson, O., Cormier, D., West, H. and Mahale, T. Properties of Ti–6Al–4V non-stochastic lattice structures fabricated via electron beam melting. *Mater. Sci. Eng. A* (2008) **492**:468-474.

[13] Tsopanos, S., Mines, R.A.W., McKown, S., Shen, Y., Cantwell, W.J., Brooks, W. and Sutcliffe, C.J. The influence of processing parameters on the mechanical properties of selectively laser melted stainless steel microlattice structures. *J. Manuf. Sci. Eng.* (2010) **132**:041011.

[14] Mahshid, R., Hansen, H.N. and Højbjerre, K.L. Strength analysis and modeling of cellular lattice structures manufactured using selective laser melting for tooling applications. *Mater. Des.* (2016) **104**:276-283.